Int. J. Chem. Sci.: 13(2), 2015, 605-612
ISSN 0972-768X
www.sadgurupublications.com

STRUCTURAL AND FERROMAGNETIC INVESTIGATION OF THE SIZE EFFECTS IN PURE AND Co DOPED SnO_2 NANO PARTICLES

M. SARAVANAKUMAR[*], S. AGILAN[a], N. MUTHUKUMARASAMY[a] and V. RUKKUMANI[b]

Department of Physics, SVS College of Engineering, COIMBATORE (T.N.) INDIA
[a]Department of Physics, Coimbatore Institute of Technology, COIMBATORE (T.N.) INDIA
[b]Department of Electronics and Instrumentation Engineering, Sri Ramakrishna Engineering College, COIMBATORE (T.N.) INDIA

ABSTRACT

Structural, micro structural and magnetic properties of pure and Co doped SnO_2 nano particles with different concentration (2%, 4% and 6%) have been studied. These nano particles synthesized by chemical precipitation method using cobalt nitrate hexahydrate $Co(NO_3)_2{\cdot}6H_2O$ and tin chloride ($SnCl_2.2H_2O$), respectively. X-ray diffraction (XRD), high transmission transmission electron microscopy (HRTEM), room temperature magnetization measured using Vibrating Sample Magnetometer (VSM) were performed to study the crystal structure, morphology and magnetic properties of Co doped SnO_2. The X-ray diffraction patterns show that all the specimen have tetragonal rutile structure without any extra phase. It reveals polycrystalline nature with prominent peaks along (110), (101), (200) and (211) planes. All the samples are nano crystalline with particle size lying in the range of 5-25 nm calculated by DS formula. HRTEM results depict the formation of spherically shaped and and particle size lies in range of 16-25 nm. SnO_2 nano particles after doped Co show ferromagnetic behavior at room temperature the coercive field (*Hc*) values are found to be increased with increase in Co doping concentrations.

Key words: Semiconductor nanoparticles, SnO_2 nanoparticles, HRTEM, Optical properties.

INTRODUCTION

Diluted magnetic semiconductors (DMS) such as Co- or Mn-doped TiO_2, ZnO, SnO_2, GaAs[1] have attracted a great deal of attention due to their great potential for novel applications in spintronics devices[2]. A fraction of the cations are replaced by magnetic ions in DMS materials because of that complex and interesting optical and magnetic properties

[*]Author for correspondence; E-mail: saranspectra@gmail.com

will be exhibited, which are tunable[3]. At the beginning of the development in this field, the DMSs based on III–V or II–VI were intensively studied, even though these materials show ferromagnetism only at very low temperatures. The magnetic behavior of such materials depends upon the concentration of the transition metal (TM) ions in the crystal, the carrier density, and the crystal quality. These are essential for spintronic device application as long as their Curie temperature does not exceed room temperature. The control of spin-dependent phenomena in DMS may lead to devices such as spin light-emitting diodes (spin-LEDs), spin field effect transistors (spin-FET), and the spin qubits for quantum computers[4,5].

SnO_2 doped with small fraction of TM ion can be a good candidate for DMS because of its vast number of structural geometries with an electronic structure that can exhibit metallic, semiconductor or insulator character[4] and wide application in polarized light emitters, chips that integrate memory and microprocessor functions, magnetic devices exhibiting gain and ultra-low power transistors, gas sensors, dye base solar cells, optoelectronic devices, electrode materials, and catalysts[6-11]. It is one of the most promising candidates for room temperature ferromagnetism (RTFM) semiconductors.

Synthesis of nano particles is a challenging task and various methods have been reported by different research groups[12-14]. The chemical precipitation method is an effective method for nanoparticle synthesis due to their high purity homogeneous material, low processing temperature and possibility of producing compositions which are not possible from other synthesis methods[15]. This method has been used by different research groups and has reported successful synthesis of nanoparticles[16].

The present work focuses on synthesizing pure and Co-doped SnO_2 powder with different concentration synthesis by chemical precipitaton method. SnO_2 doped with small amount of Co^{2+} (i.e. $Sn_{0.75}Co_{0.25}O_2$) without any modification in the structure has been of the most considerable interest. Therefore, the structural and morphological analysis of the synthesized $Sn_{1-x}Co_xO_2$ was carried out by X-ray diffraction (XRD) technique, HR TEM and Vibrating Sample Magnetometer (VSM).

EXPERIMENTAL

SnO_2 nano particles doped with three different concentration of Co (2%, 4% and 6%) were prepared by chemical co-precipitation method. The precursors for dopant and host were cobalt nitrate hexahydrate [$Co(NO_3)_2 \cdot 6H_2O$] and tin chloride [$SnCl_2.2H_2O$], respectively.

These entire chemicals were weighed in stoichiometric proportions and dissolved in 100 mL of distilled water. Then aqueous ammonia (NH_4OH) of 0.4 M was added with the

solution under constant stirring to increase the pH of the solution for the precipitate formation. After 30 min, the solution completely converted to a highly viscous gel. The solution obtained was centrifuged at 3000 rpm for 10 mins. The precipitate was filtered out separately and washed with de-ionized water for to remove unnecessary impurities formed during precipitation process. The obtained product was placed in oven for 8 h at 80^{o}C. The samples pure and cobalt doped SnO_2 with three different concentration of Co (2%, 4% and 6%) have been prepared. The obtained powders were characterized by XRD using X-ray diffractometer. This work reports on a swift chemical route to synthesize highly stable pure and Co doped SnO_2 nano particles, with different dopant concentrations and grain sizes. The synthesis procedure is highly reproducible, low-cost and easily scaled-up. The influence of the Co doping concentration with on the structure, microstructure and magnetic properties of SnO_2 the different synthesized samples was studied. The magnetic property of the samples were observed by Vibrating Sample Magnetometer.

RESULTS AND DISCUSSION

Figure 1 shows a representative set of diffractograms recorded for the synthesized pure SnO_2 and $Sn_{1-x}Co_xO_2$ nanopowder samples. The diffraction peaks were indexed on the basis of the tetragonal rutile SnO_2 phase, using the JCPDS database card no. 41-1445.[3] All the XRD patterns showed sharp diffraction peaks matching the expected diffraction reflections of the or corresponding to (110), (101), (200), (211), (220), (310), (301), (302) and (321) rutile SnO_2 planes, with similar relative intensities. No traces of other undesirable phases were observed throughout the whole range of Co contents considered, whereas the intensity of the diffraction peaks increased with increase of Co contents. Co-Sn or Co-Sn-O phases. It is clearly indicated that the incorporation of Co contents enhanced the crystallinity without affecting rutile phase of SnO_2. The XRD patterns of the obtained samples revealed the formation of cobalt doped tin oxide. Only the diffraction lines of the tetragonal rutile SnO_2 were observed without any other peaks, indicating that the Co has entered SnO_2 lattice without changing the tetragonal rutile structure.

The average crystallite size was measured using the Debye-Scherer's formula,

$$D = \frac{k\lambda}{\beta \cos\theta} \quad \ldots(1)$$

Where, D = Average size of the crystal,

λ = Wavelength of X-ray used = 1.54059 Å

K = Constant (K = 0.9),

β = Full width at the half maximum (FWHM) of the diffraction peaks

θ = The Bragg's angle

Based on the SnO_2 (110) diffraction peak the crystallite size of the SnO_2 and Co-doped SnO_2 particles were estimated. The crystallite sizes were calculated to be about 5 nm to 25 nm for the powders of SnO_2 and Co doped SnO_2, respectively. The calculated crystallite size was found to be very less than Co-doped SnO_2.

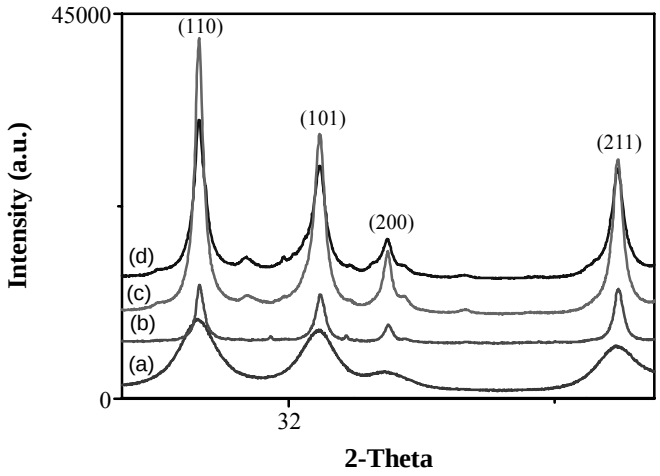

Fig. 1: The X-ray diffraction patterns of pure and Co doped SnO_2 nano particles prepared using different source concentration (a) 2% M, (b) 4% M, (c) 6% M

The morphology and structure of the nanoparticle samples were further investigated by High Resolution Transmission Electron Microscopy (HRTEM). Fig. 2(a**)** shows the Transmission Electron Microscopy of 4% Co doped SnO_2 nanoparticles of 0.4 M concentration. It is clear that sample display the aggregation of spherical nanoparticles. During co-precipitation technique, simultaneous occurrence of particle growth, nucleation and agglomeration take place[17]. Fig. 2(c) shows bright field HRTEM micrographs of a set of synthesized nanopowder samples as well as SAED images. As shown, the Co doped SnO_2 sample is composed of nanoparticles showing a *quasi*-spherical shape, Since the sample consists of a very large number of small randomly distributed particles, the SAED pattern consist of well-defined continuous diffraction rings, which can be indexed, from inside to outside, to the (110), (101), (200), (211), (220), (310), (301), (302) planes of rutile SnO_2, in accordance with XRD reflections described above. SAED images of each Co-doped samples are shown as insets in the corresponding HRTEM micrograph.

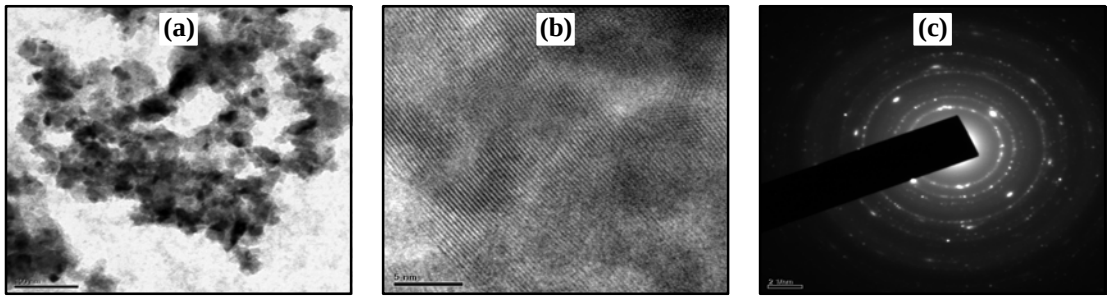

Fig. 2: HR-TEM images of the Co doped SnO_2 nanoparticles prepared using 4% doped source concentration (a) Image of nano particle (b) d-spacing (c) SAED pattern

The particle size of 2%, 4% and 6% Co doped SnO_2 nano particles has been obtained as 16 nm, 19 nm and 25 nm, respectively. The HRTEM image shown in Fig. 2(b) exhibit lattice fringes and the lattice spacing has been calculated using these fringes. The interplanar spacing of SnO_2 nanoparticle is a = 4.738 Å and c = 3.187 Å, which corresponds to the (110) plane of the tetragonal phase. The Fig. 2(c) shows the selected-area diffraction (SAED) patterns of 4% Co doped SnO_2 nanoparticles prepared using 0.4 M concentration. The selected-area diffraction patterns exhibit concentric circles, revealing that the SnO_2 samples are nano crystalline in nature and are made up of small particles. The analysis of the HRTEM images showed that Co-doped samples present similar spherical morphologies. The size of the particle was found to be in nanometer scale. Fig. 3 shows the magnetization versus applied magnetic field M-H curves SnO_2 nano particles after doped with different Co concentrations (2%, 4% and 6%) at room temperature. From the hysteresis loop, the coercive field (*Hc*) values are found to be increased with increase in Co doping concentrations as shown in Fig. 3. This enhancement in magnetization is due to the intrinsic nature of investigated samples since the structural investigation has ruled out the presence of any secondary phases. Pure SnO_2 surface has two characteristics surface sites: fivefold coordinated Sn^{4+} ions and two fold coordinated O^{2-} ions. With an addition of Co ions into the host SnO_2 matrix, Co doping introduced redundant negative charge to the lattice making the system un equilibrium in total charge. For maintaining the charge balance, an amount of O^{2-} ions need to escape from the lattice forming oxygen vacancies. These oxygen vacancies tend to locate near the Co ions[18]. The localized spins of the Co ion interact with the charge carriers, which are bound to oxygen vacancies resulting in a magnetic polarization and forming the bound magnetic polar on (BMP)[19]. A number of BMPs overlap and coalesce in to an extended ferromagnetic domain, which ultimately create the long range ferromagnetic ordering of investigated samples. As the Co concentration is increased the increase in magnetic moment is caused due to the conversion of spin-spin coupling between Co ions and it's neighbouring O atoms from anti parallel to parallel, which attributes to the

hybridization and electron transfer between oxygen vacancy state and Co-3d state[20]. The large values of Ms observed for smaller crystallite size is attributed to the large amount of induced defects and oxygen vacancies formed in the sample with Co doping.

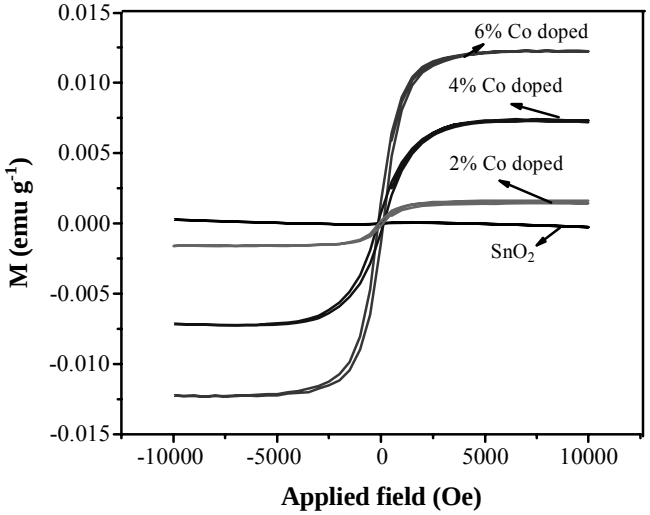

Fig. 3: M-H loop showing hysteresis of pure and Co-doped SnO_2 nano particles at room temperature magnetization (*M*) versus applied field (*H*)

These observation rule out the possibility of ferromagnetism due to unnecessary Co precipitates in the samples. In the absence of above precipitates, the observation of ferromagnetism requires exchange interaction between free delocalized carriers and localized d-spins of Co ions. Therefore, the presence of free carriers in the samples is a necessary condition for the observation of ferromagnetism. The required free charge carriers might be made available by the presence of multi valence Co ions viz. Co^{2+} and Co^{3+} as well as Valance centers. Further, increase of doping concentrations results in the annihilation of Vicente's, thereby is reducing the overall free charge carrier density.[21] As a result, the dominant magnetic interaction between Co ions becomes nearest neighbour anti-ferromagnetic and its ferromagnetic properties gradually increase after 2% Co doping concentration. Hence, to achieve the best ferromagnetic character in the materials, the concentration of Co dopant has to be properly optimized. The large values of Ms observed for smaller crystallite size is attributed to the large amount of induced defects and oxygen vacancies formed in the sample with Co doping.

At room temperature coercive field (*Hc*) and the remnant magnetization (emu/g) are observed with the increase in the doping concentration correspondingly. The reminant magnetization (emu/g) increases with the increase in the concentration, respectively. The

coercive field is constant. (*Hc* and the reminant magnetization (emu/g) can be observed respectively from the Fig. 3. The reminant magnetization (emu/g) increases with the increase in crystallite size. Room temperature ferromagnetic behavior is exhibited by the $Sn_{1-x}Co_xO_2$ samples.

CONCLUSION

We have successfully synthesized pure and Co (2, 4, and 6 wt.%) doped SnO_2 nanoparticles by the chemical co-precipitation method. The rutile structure of SnO_2 was confirmed by X-ray diffraction and HRTEM studies and no presence of Co metals or other magnetic phases could be detected. Pure and Co doped SnO_2 nanoparticles exhibit room temperature ferromagnetism, which was attributed to the possible enhancement of oxygen vacancies in the parent compound SnO_2. The saturation magnetization (Ms) and coercive field (H_C) of Co (2,4,6 wt.%) doped SnO_2 nanoparticles are found to be about 1.8 x 10^{-4} g, 2.65 x 10^{-3}, 3.08 x 10^{-3} emu g and 223 kOe, respectively and the saturation magnetization (Ms) increased with increase in Co doping concentrations.

REFERENCES

1. L. Yan, J. S. Pan and C. K. Ong, Mat. Science Eng, B, **128**, 34-36 (2006).
2. M. Luo, F. Sun, Optik, **125**, 2157-2159 (2014).
3. K. Ueda, H. Tabata and T. Kawai, Appl. Phys. Lett., **79**, 988 (2001).
4. M. S. Arnold, P. Avouris, Z. W. Pan and Z. L. Wang, J. Phy. Chem. B, **107**, 659 (2003).
5. D. D. Awschalom and M. E. Flatté, Nat. Phys., **3**, 153 (2007).
6. J. Kaur, J. Shah, R. K. Kotnala and K. C. Verma, Ceramics International, **38**, 5563 (2012).
7. K. Y. Kim, E. R. Kim, K. Y. Han, K. H. Nam and D. W. Ihm, Jpn. J. Appl. Phys., **41**, 237 (2002).
8. E. Comini, G. Faglia, G. Sberveglieri, Z. Pan and Z. L. Wang, Appl. Phys. Lett., **81**, 1869 (2002).
9. F. Gu, S. F. Wang, M. K. Lu, Y. X. Qi, G. J. Zhou, D. Xu, D. R. Yuan, Opt. Mater., **25**, 59 (2004).
10. S. Mehraj, M. Shahnawaze Ansari, Alimuddin, Physica B, **430**, 106-113 (2013).

11. T. Hayakawa and M. Nogami, Sci. Technol. Adv. Mater., **6**, 66 (2005).

12. S. Ferrere, A. Zaban and B. A. Gsegg, J. Phys. Chem. B, **101**, 4490 (1997).

13. C.-H. Yu, K. Tam and E. S. C. Tsang, Handb. Met. Phys., **5**, 113 (2008).

14. S. Das, S. Basu, G. Majumdar, D. Chakravorty, S. Chaudhuri and J. Nanosci. Nanotechnol, **7**, 4402 (2007).

15. H. Yang, X. Song, X. Zhang, W. Ao and G. Qiu, Mater. Lett., **57**, 3124 (2003).

16. F. Gu, S. F. Wang, M. K. Lü, G. J. Zhou, D. Xu and D. R. Yuan, J. Phys. Chem. B, **108**, 8119 (2004).

17. L. M. Sikhwivhilu, S. K. Pillai and T. K. Hillie, J. Nanosci. Nanotechnol., **11**, 4988 (2011).

18. F. Gu, S. F. Wang, M. K. Lü, G. J. Zhou, S. W. Liu, D. Xu and D. R. Yuan, Chem. Phys. Lett., **372**, 451 (2003).

19. J. M. D. Coey, M. Venkatesan and C. B. Fitzgerald, Nat. Mater., **4**, 173 (2005).

20. C. F. Yu, T. J. Lin, S. J. Sun, H. Chou, J. Phys. D: Appl. Phys., **40**, 6497-6500 (2007).

21. H. Jiang, X. F. Liu, Z. Y. Zou, Z. B. Wu, B. He and R. H. Yu, Appl. Surf. Sci., 258, 236 (2011).

Revised : 30.01.2015 *Accepted : 31.01.2015*